Digitally-programmable manufacturing of living materials grown from biowaste

*Suitu Wang, Laura K. Rivera-Tarazona, Mustafa K. Abdelrahman, Taylor H. Ware**

S. Wang, M. K. Abdelrahman, Prof. T. H. Ware

Department of Materials Science and Engineering

Texas A&M University

College Station, TX77843, USA

Correspondence: taylor.ware@tamu.edu

L. K. Rivera-Tarazona, Prof. T. H. Ware

Department of Biomedical Engineering

Texas A&M University

College Station, TX77843, USA

Keywords: engineered living materials, bread waste, biomass, degradable polymers, biomanufacturing, shape change

Abstract

Materials manufacturing strategies that use little energy, valorize waste, and result in degradable products are urgently needed. Strategies that transform abundant biomass into functional materials

form one approach to these emerging manufacturing techniques. From a biological standpoint, morphogenesis of biological tissues is a "manufacturing" mode without energy-intensive processes, large carbon footprints, and toxic wastes. Inspired by biological morphogenesis, we propose a manufacturing strategy by embedding living *Saccharomyces cerevisiae* (Baker's yeast) within a synthetic acrylic hydrogel matrix. By culturing the living materials in media derived from bread waste, encapsulated yeast cells can proliferate resulting in a dramatic dry mass and volume increase of the whole living material. After growth, the final material is up to 96 wt% biomass and 590% larger in volume than the initial object. By digitally programming the cell viability through UV irradiation or photodynamic inactivation, the living materials can form complex user-defined relief surfaces or 3D objects during growth. Ultimately, the grown structures can also be designed to be degradable. The proposed living materials manufacturing strategy cultured from biowaste may pave the way for future ecologically friendly manufacturing of materials.

1. Introduction

Manufacturing of polymeric materials has enabled products that are ubiquitous in modern society.[1] However, traditional manufacturing of polymeric materials relies on valuable precursors derived from fossil fuels,[2] and energy-intensive manufacturing procedures.[3] As a result, nearly 4% of global carbon emissions can be attributed to the lifecycle of polymers.[4] Furthermore, synthetic polymeric waste continually accumulates in the environment as less than 10% of all plastics are recycled, and this waste persists for many years.[5,6] Numerous efforts are aimed at addressing these critical issues, including work focusing on deriving precursors from renewable sources,[7–10] manufacturing goods with low-energy processes,[11,12] and designing polymers to be compostable.[13,14] Despite these significant advances, the above problems still

remain. Future approaches to "eco-manufacturing" of polymer composites are needed to address these concerns.

Eco-manufacturing should enable the utilization of natural, bio-sourced, recyclable, or waste materials as precursors to transform low-cost, sustainable resources into material production. One major source of waste comes from food production. For example, millions of tons of bread are wasted annually, due to limited shelf life or unsatisfactory products during baking.[15] Strategies to recycle bread waste have been investigated for decades, including using bread waste directly as feedstocks for microbial growth. Through specific enzymatic processes or bacterial fermentation, bread waste can be utilized for the production of succinic acid,[16] lactic acid,[17] ethanol,[18] or enzymes.[19] Such methods can potentially reduce the amount of bread waste disposal in landfills. Strategies to utilize bread waste as a substrate to make growth media for yeast cultivation have also been proposed.[20,21] The idea of transforming abundant biowaste into biomass production is intriguing. However, a bridge transforming biomass production into functional products is still lacking.

Eco-manufacturing strategies should consider not only the production of the polymeric material but also the forming of the material into the product. Additive manufacturing of polymers has led to a new era of near net shape manufacturing, enabling new designs, utilizing low energy processes, and reducing waste of starting materials.[22,23] Morphogenesis of biological tissues can be considered as an "additive manufacturing" process where living organisms assemble biomass to form a wide variety of 3D tissues. This process is usually powered by chemical or solar energy present in the environment, which stands in stark contrast to the energy-intensive processes used for synthetic materials production. However, most organisms do not intrinsically produce materials in forms suitable for engineering applications.

Engineered living materials (ELMs) are composites where living cells are combined with synthetic materials.[24–30] The resulting living materials derive functionalities from biological activities while keeping material properties for engineering applications.[31–36] One class of ELMs focuses on functionalities directly from the biochemical activities of the living cells, including fungal-based self-cleaning living surfaces that metabolize food spills,[37] 3D printed bacterial structures as living electrodes,[38] yeast-laden living hydrogels for continuous biofermentation,[39] and encapsulated bacteria as wearable sensors.[40] Another approach in ELMs is to utilize the biochemical activities of living cells to control the mechanical properties of the living materials or produce functional materials.[41–45] For example, dried yeast themselves can serve as building blocks of stiff materials,[46] and mycelia can adhere sawdust into solid objects.[47–49] Bacteria-assisted mineralization can help self-heal concrete or improve the toughness of 3D-printed polymer scaffolds.[50] Engineered microbial biofilms can be directly used for the fabrication of biodegradable bioplastics.[51] Co-cultures of bacteria and yeast, similar to those used to create the drink Kombucha, can create materials based on bacterial cellulose from nutrients found in the growth media.[52] Our previous work has also shown that living materials comprised of yeast encapsulated in a synthetic hydrogel can grow into 3D structures due to patterned cell proliferation.[53] However, in these cases, hydrogels of relatively simple shapes were the final product of the growth. Furthermore, the final materials were not degradable, and growth was fueled with expensive laboratory media. A living material system where growth fueled by waste yields complex 3D objects that can ultimately degrade would enable a new route to eco-manufacturing of polymers.

Herein, we report an eco-manufacturing approach utilizing the fabrication and patterned growth of living materials (**Scheme 1**). Yeast embedded within a synthetic hydrogel matrix grow

into patterned forms, yielding materials that are > 96% biomass and have adopted a programmed 3D form. One feature of this approach is the valorization of bread waste as growth media for the living materials, which allows the transformation of abundant wasted biomass into useful materials. Using patterned light, the local concentration of living yeast can be varied, leading to patterned growth and enabling digital control of the shape that is adopted after growth. Grown and dried living materials can be directly used in load-bearing structures or as relief surfaces due to tunable elastic moduli comparable to synthetic engineering polymers. Ultimately, these materials can be designed to be fully degradable at the end of life. The described approach will enable an alternative eco-manufacturing paradigm for future manufacturing of materials.

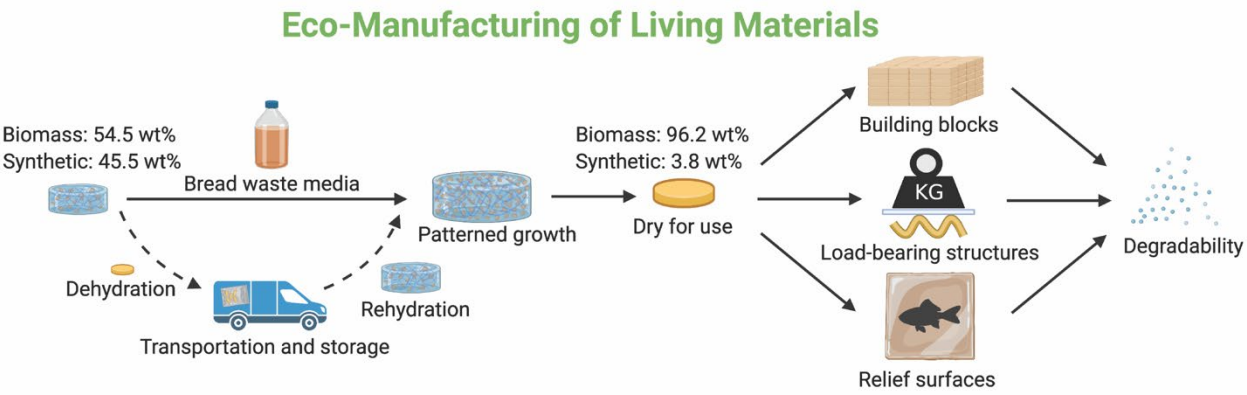

Scheme 1. Schematic of the eco-manufacturing process based on the growth of living materials.

2. Experimental Section

Materials. 2-Hydroxyethyl acrylate (HEA), acrylamide (AM), *N,N'*-methylenebisacrylamide (MBAm), poly(ethylene glycol) diacrylate (PEGDA) (700 g mol^{-1}), n-butylamine, protease from *Aspergillus oryzae* (≥ 500 U g^{-1}), amyloglucosidase from *Aspergillus niger* (70 U mg^{-1}), α-amylase from Aspergillus oryzae (≥ 150 U mg^{-1}), pentaerythritol tetrakis(3-mercaptopropionate) (PETMP), ammonium persulfate (APS), N,N,N',N'-tetramethylethane-1,2-diamine (TEMED),

toluene, and 3-(trimethoxysilyl)propyl methacrylate were all purchased from Sigma Aldrich. Rain-X and commercial yeast (S. cerevisiae, active dry yeast, Fleischmann's) were purchased from Walmart (College Station, TX). Yeast extract-peptone-dextrose (YPD) was purchased from Fisher Scientific. Nature's Own 100% whole wheat bread was purchased from Sam's Club (College Station, TX). Triallyl isocyanurate (TATATO) was purchased from TCI Chemicals. Irgacure I-369 was donated by BASF. 7,12-*bis*(1-hydroxyethyl)-3,8,13,17-tetramethyl-21H,23H-porphine-2,18-dipropanoic acid, dihydrochloride (hematoporphyrin) was purchased from Cayman Chemical. All chemicals were used as received without further purification.

Bread waste media preparation. Old but not spoiled bread waste expired from 1 to 8 weeks (50 g) was ground and mixed with distilled water (200 mL) in a 250 mL glass flask. The mixture was kept at 60 °C for 15 minutes to enable gelatinization. Amylolytic and proteolytic enzymes: α-Amylase from Aspergillus oryzae (≥ 150 U mg^{-1}) (Sigma Aldrich) (10 mg), amyloglucosidase from *Aspergillus niger* (70 U mg^{-1}) (Sigma Aldrich) (14 mg), and protease from *Aspergillus oryzae* (≥ 500 U g^{-1}) (Sigma Aldrich) (3 μL) were then added to the mixture and maintained at 60 °C for 12 hours to enable hydrolysis of bread waste into amino acids and sugars. Extracts were then centrifuged at 4000 rpm for 10 minutes. The obtained supernatants were sterilely filtered using Fisherbrand sterile disposable vacuum filter units with 0.2 μm sized polyethersulfone (PES) membranes.

Glass molds preparation. For making free-standing living materials, two glass slides treated with Rain-X were assembled with 1 mm spacers. Parafilm was used to wrap one side of the glass molds with another side open for solution filling. For living materials attached on a glass slide, glass slides functionalization was conducted. Briefly, sterile glass slides were kept in deionized water overnight to keep the surface hydrated, soaked in a 5 vol% solution of 3-

(trimethoxysilyl)propyl methacrylate in toluene at 60 °C for 30 minutes, washed with toluene, dried with nitrogen gas, and baked at 120 °C for 5 minutes. Then one functionalized glass slide was assembled with another Rain-X treated glass slide with 1 mm spacers. The molds were wrapped with parafilm while leaving one side open for solution filling.

Bis-PEGDA synthesis. 1 : 2 molar ratio of n-butylamine and PEGDA were mixed together, reacted at 65 °C for 24 hours to finish the Michael addition reaction.

Living materials preparation. All living materials were prepared at room temperature by free radical polymerization. To make PHEA living materials, 10 wt% HEA and 0.1 wt% MBAm were dissolved in deionized water to form precursor solutions. Then 12 wt% yeast (~4 billion cells mL^{-1} of the monomer solution) were added to the solution and mixed for 30 seconds to form a uniform dispersion, followed by the addition of 0.1 vol% APS and 0.1 vol% TEMED. The dispersion was mixed for 3 seconds and quickly pipetted into glass molds. The filled molds were turned over every 30 seconds during polymerization to avoid yeast sedimentation. After polymerizing for 5 minutes, the resultant samples were demolded and washed with deionized water three times to remove the unreacted monomers. Then the samples were soaked in deionized water overnight to reach swelling equilibrium before growth. To prepare other living materials with different monomer ratios, 10 wt% HEA was replaced with 5 wt% HEA and 5 wt% acrylamide or with 10 wt% acrylamide to form the precursor solutions. To make other living materials with different crosslinkers, MBAm was replaced with same mole percent of PEGDA (700 g mol^{-1}) or Bis-PEGDA (1473.14 g mol^{-1}) to form the precursor solutions.

Measurement of volume change, and mass change of the living materials. Living materials were cut into disks with 10 mm diameter after equilibration in DI water. The disks were photographed with a Canon Rebel T5i camera, and the dimensions were measured by

ImageJ. Samples were cultured in same volume of YPD or bread waste media (10 disks every 150 mL media) at 30 °C in a shaking incubator at 200 rpm. The media was renewed every 24 hours. Volume change and wet mass change were measured every 24 hours for 96 hours. To measure dry mass change, initial and grown samples were dried at 60 °C for a day to allow water evaporation. Dry mass change was measured every 24 hours for 96 hours. $n \geq 10$. The square living material growth parameters were identical to the disk growth parameters. The large (5 cm × 6 cm) samples were cultured individually in 200 mL of bread media. The media was refreshed every 12 hours for 4 days.

Living material structures. 1) Large (5 cm × 6 cm) samples were assembled using adhesive tape. 2) More than 200 square living materials were tiled, and each layer was coated with a 1:1 weight ratio of PETMP and TATATO with 0.5 wt% I-369. The layers were then photopolymerized with UV light. 3) For the unstructured slurry, same biomass ratio of dry yeast was mixed with the PETMP/TATATO/I-369 solution and then photopolymerized with UV light. Poor dispersion of high content of yeast in the monomer solution resulted in a slurry of yeast agglomerates.

Scanning electron microscopy (SEM) images of living materials. Dried samples before and after growth were prepared by sputtering a 15 nm layer of Au. Images were taken using a NeoScope JCM-5000 SEM operating at 10 kV. To build grown structures, living materials were either cut in 1 cm × 1 cm or 5 cm × 6 cm pieces.

Thermogravimetric analysis (TGA) of living materials. Dried samples (10 mg) before and after growth were run at 30 °C min^{-1} under N_2 purging at 40 mL min^{-1} using a TA TGA Q50 instrument ($n = 3$).

Dynamic mechanical analysis (DMA) of living materials. Dried samples (20 mm × 3 mm × 1 mm) before and after growth were tested in tensile mode by using a TA RSA-G2 instrument. Samples were tested at 0.1% strain at 1Hz and heated from -20 °C to 120 °C at a rate of 3 °C min^{-1} (n = 4).

Tensile test of living materials. Tensile testing was conducted using an Instron 3345 equipped with a 10 kN load cell. Testing was performed at room temperature. Dried rectangular samples were cut before and after growth with dimensions (approximately 40 mm length × 5 mm width × 1 mm thickness). Each sample was placed between two clamps and stretched at a fixed deformation rate (5 mm min^{-1}) until breaking. The elastic modulus was calculated by using the first 0.3% strain (n = 4).

Accelerated degradation test of living materials. Living materials were cut into 10 mm-diameter disks and cultured for 4 days. Both initial and grown living materials with different crosslinkers were soaked in 33 mM NaOH solutions at 37 °C. Same number of samples with different crosslinkers were dried and measured the remaining dry mass every 24 hours. Dry mass remaining is calculated by the ratio of remaining mass to original mass ($n \geq 10$).

Dry and grow test of living materials. Initial living materials were dried in the vacuum chamber at room temperature for 2 days. Dried samples were stored in the bench drawer at room temperature for the specified time. Then samples were soaked in deionized water for 1 day to reach swelling equilibrium and cultured for 4 days. The maximum volume change, wet mass change, and dry mass change of the grown living materials were measured ($n \geq 10$).

Statistical analysis. Analysis of the normality and variance showed normal data with equal variance. Statistical comparisons were made using the 1-way ANOVA test followed by a post-hoc Tukey test.

UV photopatterning of living materials. Living material films were soaked in deionized water to reach swelling equilibrium before UV exposure. Shadow masks with different shapes were designed by AutoCAD and laser cut from black polymer sheets. For the "TAMU" and "fish" patterns, the samples were exposed to UV (254 nm) irradiation with an intensity of 2 mW cm^{-2} for the living material film with one side covered with the corresponding photomask for 40 minutes while the other side uncovered for 40 minutes using an UVP UVLink 1000 cross-linker chamber. For the corrugated pattern, UV irradiation was performed using four rectangular photomasks with placed at a regular interval. The masks were placed such that each region of the film was exposed on either the top or bottom. Irradiation was performed 40 minutes on each side. After irradiation, films were cultured in bread waste media at 30 °C for 2 days and dried at 60 °C for 1 day. Similarly patterned samples were fabricated at least 3 times to confirm the reproducibility of the deformation.

Compression test. Compression testing was conducted using an Instron 3345 equipped with a 20 kN load cell. Testing was performed at room temperature. Corrugated specimen with dimensions (approximately 15 mm length × 6 mm width × 5 mm height) was placed between two steel plates and compressed at a fixed deformation rate (1 mm min^{-1}) until reaching the maximum 1 kN force to obtain the force-strain curve (n = 4).

Visible light photopatterning of living materials. Living material films covalently bound to methacrylate-functionalized glass slides were soaked in 20 mM hematoporphyrin (photosensitizer) aqueous solutions overnight. The dyed films were exposed to white light from a modified projector with an intensity of 460 W m^{-2} for 20 minutes in the air. Different grayscale photos were displayed by the Vivitek projector to spatially control the actual light intensity that the films received. After exposure, films were cultured in bread waste media at 30 °C for 1 day

and dried at room temperature for 2 days. Similarly patterned samples were fabricated at least 3 times to confirm the reproducibility of the deformation.

Topography measurements of photopatterned living material films. Topography of the patterned living material films was imaged by the Nikon optical microscope. Z-stack topographical images were captured of the films. For the same dose of light, the film thickness was measured from 4 random spots among these regions in one film ($n \geq 3$).

3. Results and Discussion

Traditional manufacturing of materials allows the transformation of raw materials into user-defined shapes and products with desirable properties. Future manufacturing strategies should retain the versatility of the traditional processes while minimizing resource and energy consumption. Finally, products should degrade into benign components after use.

3.1. Biowaste to biomass through living materials growth. Utilizing biowaste as precursors for material production is a long-lasting goal. Living materials comprised of Baker's yeast and a hydrogel matrix can grow in mass and volume when cultured in media that allows for cell proliferation.[53] We hypothesized that this volume and mass increase could be considered as a manufacturing process where waste is used to fuel material growth and form adoption. Here, we synthesized living materials by radical polymerization in water of water-soluble acrylic monomers and crosslinkers in the presence of commercially-available freeze-dried, viable yeast. The resulting living materials were cultured in media derived from bread waste and laboratory yeast extract-peptone-dextrose (YPD) media under the same conditions (**Figure 1**A). The results show that living materials dramatically grow in volume and mass in both media (Figure 1B). Living materials cultured in bread waste media undergo a final volume increase of 590.9 ±

49.5% after 4 days, which is 1.5 times larger than those cultured in YPD (Figure 1C). The final dry mass increase of the living materials cultured in bread waste media is 942.8 ± 35.2% (Figure 1D and 1E), which is also ~ 1.5 times larger than those cultured in YPD. The above results indicate that bread waste may be a nutrient-rich wasted resource that can be recycled for living materials cultivation.

The increased volume and mass of the living materials due to biological growth also represents a low energy manufacturing process. Instead of using chemical reactions or melt processes to achieve the desired size and mass of the objects, living materials increase in volume and mass through in-situ proliferation of cells powered by chemicals found in the culture media. After culture in bread waste media for 4 days, the biomass of the dried living materials increases from 54.5 ± 2.0 wt% to 96.2 ± 2.9 wt%. The living materials begin with well-dispersed yeast within the polymer matrix. After growth and drying, colonies of yeast can be observed on the surface and cross-section of the living materials (Figure 1F and 1G). Individual cells also tend to protrude from the polymer matrix due to proliferation, leaving some holes on the surface (Figure S1, Supporting Information). The mechanical properties of the grown living materials are similar to a glassy polymer due to the rigid cell wall around each yeast cell.[54] These properties are further discussed below.

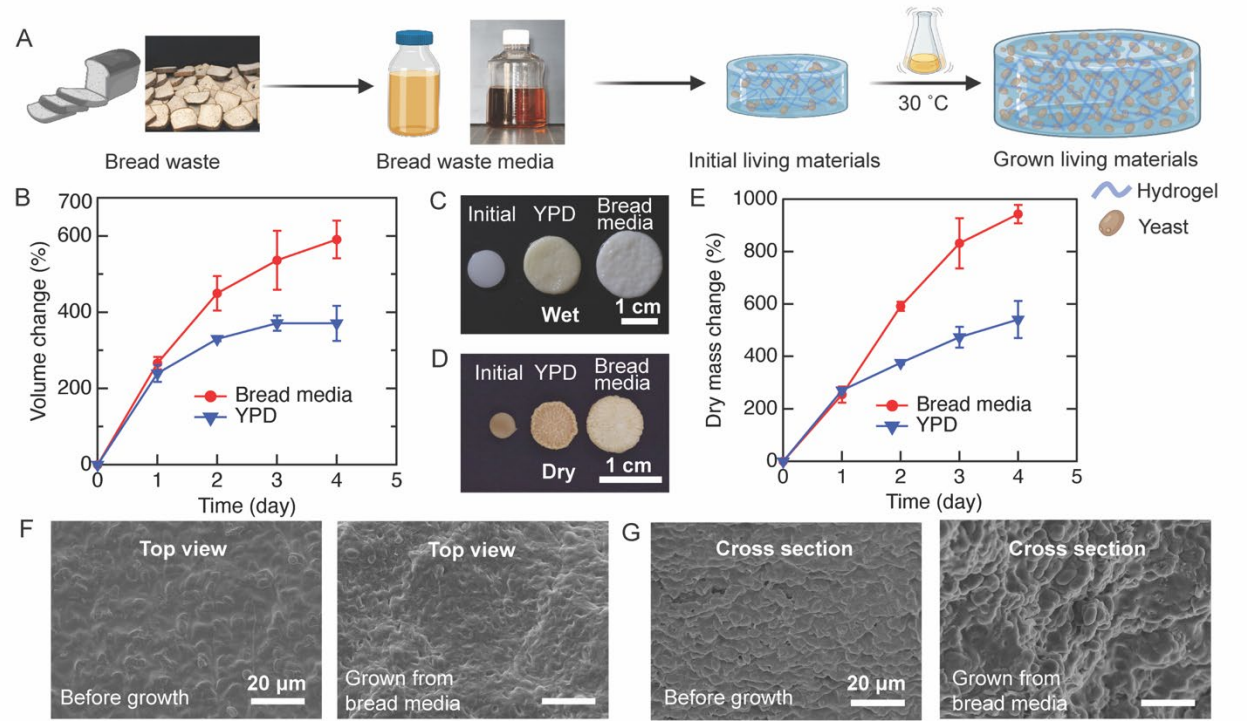

Figure 1. A) The illustration of the self-growing living materials process based on bread waste. B) Comparison of volume change of the living materials cultured in YPD and bread waste media as a function of time ($n \geq 10$). Photographs of the C) hydrated and D) dried living materials before and after growth for 4 days in two media. E) Comparison of dry mass change of the living materials cultured in YPD and bread waste media as a function of time ($n \geq 10$). SEM images showing the F) top view and G) cross-section view of the dried living materials before and after growth. Each data point represents the mean, and error bars represent SD. Trend lines are only intended to guide the eye.

3.2. Tunable material properties of grown living materials. A key advantage of using composites of synthetic polymers and living organisms for manufacturing is that traditional materials formulation approaches can be used to tune the material properties of the living materials. To demonstrate this tunability, we synthesized living materials with hydrogel matrices

comprised of acrylamide (AM), 2-hydroxyethyl acrylate (HEA), and copolymers of the two, where each of the materials is crosslinked with *N,N′*-methylenebisacrylamide (MBAm) (**Figure 2**A). The volumetric growth curve of each living material as a function of time is similar, although there is a slight decrease in the volumetric growth as the composition of acrylamide increases (Figure 2B). This result is not surprising because a certain loss of yeast cell viability entrapped in polyacrylamide (PAM) gels has been previously reported.[55–58] A similar trend is observed for the dry mass increase between living materials of different compositions (Figure 2C). To understand the thermal stability of the dried living materials, thermogravimetric analysis (TGA) is conducted. Each of the living materials is relatively resistant to thermal degradation before (Figure 2D) and after growth (Figure 2E). Interestingly, the high biomass content has little effect on the thermal degradation behaviors of the living materials. There is a slight increase in mass loss near 180 °C for the grown living materials, which may be attributed to the partial thermal degradation of yeast cells. We note that these extreme heating processes likely completely kill the embedded yeast, preventing further growth in these materials.

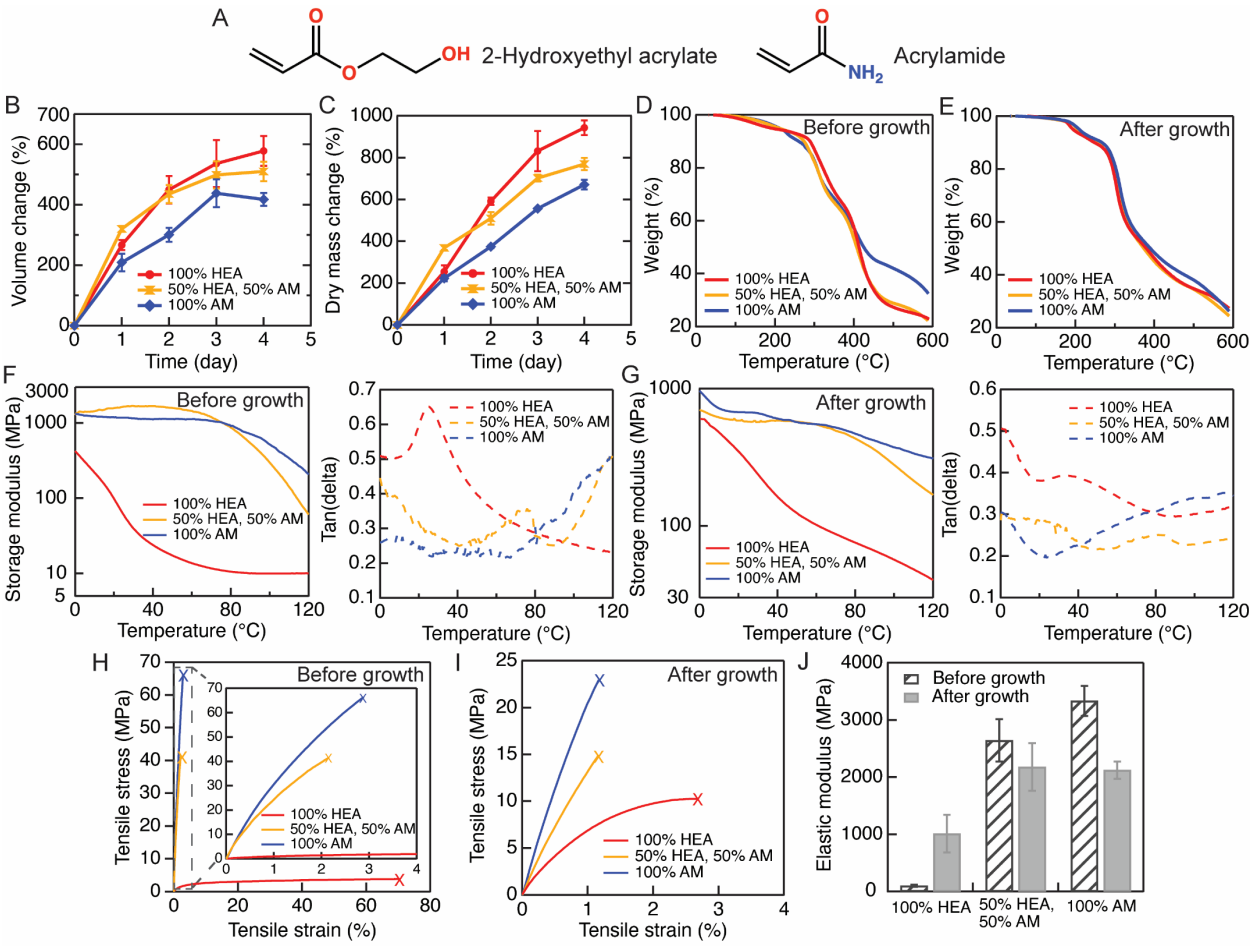

Figure 2. A) Chemical structures of different monomers that are used in the living material system. B) Volume change and C) dry mass change of the living materials cultured in bread waste media for 4 days by varying the different monomer ratio (n ≥ 10). Representative curves of thermal degradation of the different living materials D) before and E) after growing in bread waste media for 4 days (n = 3). Representative curves showing the storage modulus and glass transition temperature of the different living materials F) before and G) after growth (n = 4). Representative stress-strain curves at room temperature of the different living materials H) before and I) after growth. J) Elastic modulus of the different living materials before and after growth (n = 4). Each data point represents the mean, and error bars represent SD. Trend lines are only intended to guide the eye.

The chemical tunability of the polymer matrix enables controllable mechanical properties of living materials during manufacturing. Before growth and in the dry state, the storage modulus of living materials is strongly dependent on the polymer matrix. Due to the high glass transition temperature (T_g) of PAM, the initial living materials formed from the polymerization of AM or copolymerization of HEA and AM matrix show much higher storage modulus than the materials formed from the polymerization of HEA across the entire tested temperature range (Figure 2F).[59–62] The storage modulus at 25 ˚C of the initial living materials can be varied from 94.6 ± 54.2 MPa to 2041.1 ± 350.5 MPa by tuning the monomer ratios. This difference can be attributed to the glass transition of the polymer matrix. In the living materials comprised of poly(2-hydroxyethyl acrylate) (PHEA), the T_g is 25 °C, as measured by dynamic mechanical analysis (DMA). After growth, the storage moduli of the living materials change. As shown in Figure 2G, the storage modulus of the grown dried living materials with PAM matrix or copolymer matrix decreases while the storage modulus of the living materials with PHEA matrix increases. The modulus of the grown dried living materials varies from 296.1 ± 23.0 MPa to 948.5 ± 131.6 MPa at room temperature based on the polymer matrix. The tan(delta) peaks of grown living materials are lower than those of the as fabricated living materials, which is likely be due to the lower fraction of polymer matrix after growth. There is little shift for the tan(delta) peak position as a function of temperature before and after growth. Tensile testing demonstrates that the flexible and stretchable dried living materials with PHEA matrix before growth transform into more rigid and brittle materials after growth (Figure 2H and 2I). This change could be leveraged to grow structures with patterned mechanical properties. In comparison, growth has little effect on the stretchability of dried living materials with the other two matrices due to the high T_g of these

living materials. The elastic modulus of the living materials with PHEA matrix increases from 101.8 ± 17.7 MPa to 1013.2 ± 329.9 MPa at room temperature (Figure 2J). Living materials with PAM matrix or copolymer matrix have decreased elastic moduli from 3335.3 ± 261 MPa to 2120.7 ± 152.4 MPa and from 2642.6 ± 369.8 MPa to 2178.3 ± 416.9 MPa, respectively. This convergence of elastic moduli of living materials after growth can likely be attributed to the increased biomass as the elastic modulus of a single yeast cell is around 185 ± 15 MPa according to previous reports.[54,63] Also recently, a similar hard and stiff dried living material with elastic modulus of several GPa has been fabricated using only microbial cells.[46] Below, each described living material is fabricated with the PHEA matrix.

3.3. Dried living materials growth after storage. As yeast is readily available for home cooking in a dried state, we hypothesized that the living materials could be dried for storage after fabrication, but before growth.[64] The ability to dry and rehydrate these materials would significantly reduce storage and shipping costs in future manufacturing processes. Living materials were dried under vacuum at room temperature, stored in the dark under laboratory conditions, and then rehydrated and cultured. As shown in **Figure 3**A, these dehydrated living materials can grow after one week of storage. To quantify the extent of growth, dehydrated living materials are stored for one day or one week and then placed in bread waste media. The final volume change, wet mass change, and dry mass change are collected (Figure 3B). After being dried for one day, rehydrated, and grown, the final volume and mass change of the living materials decreases moderately compared with the original samples, which indicates that the drying and rehydrating process may lead to a loss in viability of some of the embedded yeast. However, the final dry mass change can reach up to 810.3 ± 83.4%, which is also not significantly different from the original samples by statistical analysis (P = 0.078, 1-way

ANOVA test followed by a post-hoc Tukey test). After storing for one week, the final dry mass change can reach up to 650.4 ± 60.3%. Although this difference is significant ($P < 0.001$, 1-way ANOVA test followed by a post-hoc Tukey test), the final dry mass change of the rehydrated living materials cultured from bread waste media is still larger than that of the original living materials cultured from YPD that were not subjected to the drying process. After storing for two weeks, almost no volume change is observed for the grown living materials, indicating most of the embedded cells are rendered inviable by these storage conditions. As freeze-dried yeast is typically stable for months, altered storage conditions may increase the viability of these living materials in the dried state.[44]

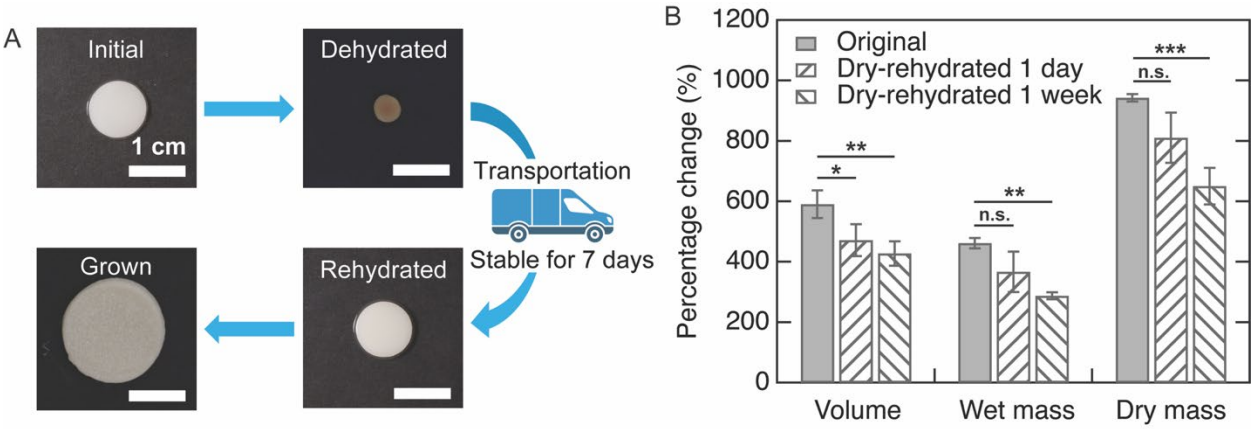

Figure 3. A) Photographic illustration showing the growth capability of the living materials after dehydration and storage in the dry state for a week. B) Comparison of the volume change, wet mass change, and dry mass change of the original and dry-rehydrated living materials after growth (n ≥ 10; *, $P < 0.05$; **, $P < 0.01$; ***, $P < 0.001$).

3.4. Grown living materials as building blocks or load-bearing structures. To demonstrate that the grown objects can be directly used to build structures with a high biomass content, more than 200 square living materials are grown, dried, and assembled with an adhesive to form a 3D

structure (**Figure 4**A). Each grown dried object is approximately 1 cm on the longer sides. The 3D structure is stable enough to support a 1 kg weight (Figure S2, Supporting Information). Notably, 85.1 wt% of the entire structure is yeast, with ~96 wt% yeast comprised in each substructure and a synthetic polymeric adhesive forming the entire structure. The process of growing the living materials yields much higher biomass in the object, which cannot be achieved from simply dispersing cells in a synthetic polymer. As an illustration, when a slurry is made with 85.1 wt% yeast and synthetic monomers, the yeast cannot be dispersed resulting in a useless paste.

Scaling up the size of building blocks plays an essential role in future manufacturing applications. By increasing the initial size of living materials and following the same culture conditions, a much larger grown dried object can be obtained (~5 × 5.8 cm in plane) with ~94 wt% biomass (Figure 4B). A simple structure can be built by assembling these larger building blocks. Larger samples may experience gradients in growth or warping during drying, which can distort the final dried state.

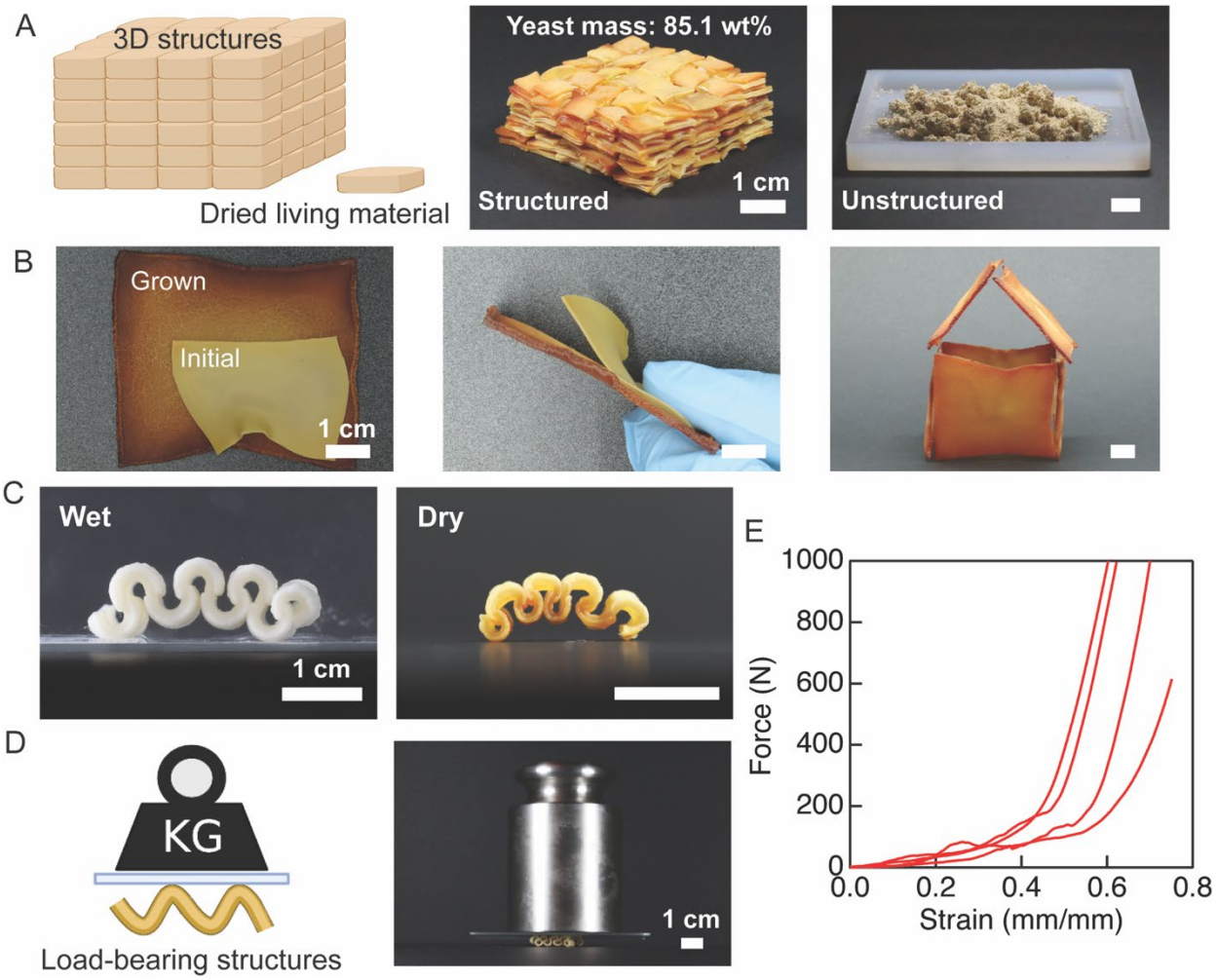

Figure 4. A) An illustration and photographs showing that the grown dried living materials can be directly used as building blocks to fabricate 3D structures. B) Photographs showing that larger grown dried objects can be obtained by scaling up the initial size of living materials, which can also be used as building blocks to build a simple structure. C) Corrugated 3D structures formed by alternating the viable cell region from top to bottom and retained after drying ($n \geq 3$). D) An illustration and an example showing that two resulting corrugated shapes (0.5 g) can be used as load-bearing structures to hold a 1 kg weight. E) Destructive compression test for one corrugated structure ($n = 4$).

Manufacturing of useful goods requires not only the production of material, but the forming of that material. Previously, we showed that spatially-controlled biological growth could be used to create living material objects with spatially-heterogeneous volume change in hydrogels.[53] The principle of using spatially-heterogeneous volume change has been applied to generate hydrogels that adopt a 3D form during swelling.[65–68] A key difference of this approach, compared to work in hydrogels undergoing swelling, is that solid biomass is responsible for the volume change, which enables the grown form to be retained after drying. Spatial control of growth can be obtained by using light to kill the embedded yeast locally. Living materials were exposed to 254 nm UV light through a shadow mask in the form of the letters "TAMU" or a simple fish (Figure S3, Supporting Information). During growth, the regions that were not exposed to light undergo a volume increase that is retained in the dry state. Dry film height differences are observed using SEM between grown and inactivated regions (Figure S3, Supporting Information). As the patterned growing region alternates from the top to the bottom surface, 3D corrugated structures can be manufactured through growth and retained after drying (Figure 4C). Due to the increased modulus after growth, the 3D corrugated structures can be used as load-bearing structures (Figure 4D). Two structures (0.5 g) easily support a 1 kg mass without substantial deformation. Destructive compression test shows the maximum crushing force that one corrugated structure (0.25 g) can withstand before being flattened is 125 ± 14 N (Figure 4E).

3.5. Digital manufacturing of living materials. Digital control of manufacturing is common in additive manufacturing. However, it is challenging to generate grayscale patterns using 254 nm UV light with conventional optical tools. As such, we sought to use a process used in medicine to treat fungal infections and cancer treatments to pattern yeast viability with visible light, photodynamic therapy.[69,70] Photodynamic therapy is a process by which cells are

inactivated in the presence of photosensitizers and visible light due to the photoinduced production of singlet oxygen ($^1O_2$).[71,72] The photosensitizer (hematoporphyrin) was swollen into living materials. The key advantage of this approach is that visible light is used, which means many common tools can be used to spatially control irradiated light intensity. This programming strategy can be applied to manufacture delicate graphic structures. A QR code relief surface can be manufactured and successfully scanned by the WeChat app in the wet state (**Figure 5**A). The QR code shape still retains but becomes unscannable in the dry state, which may enable delivering messages in a controllable and dynamic manner.

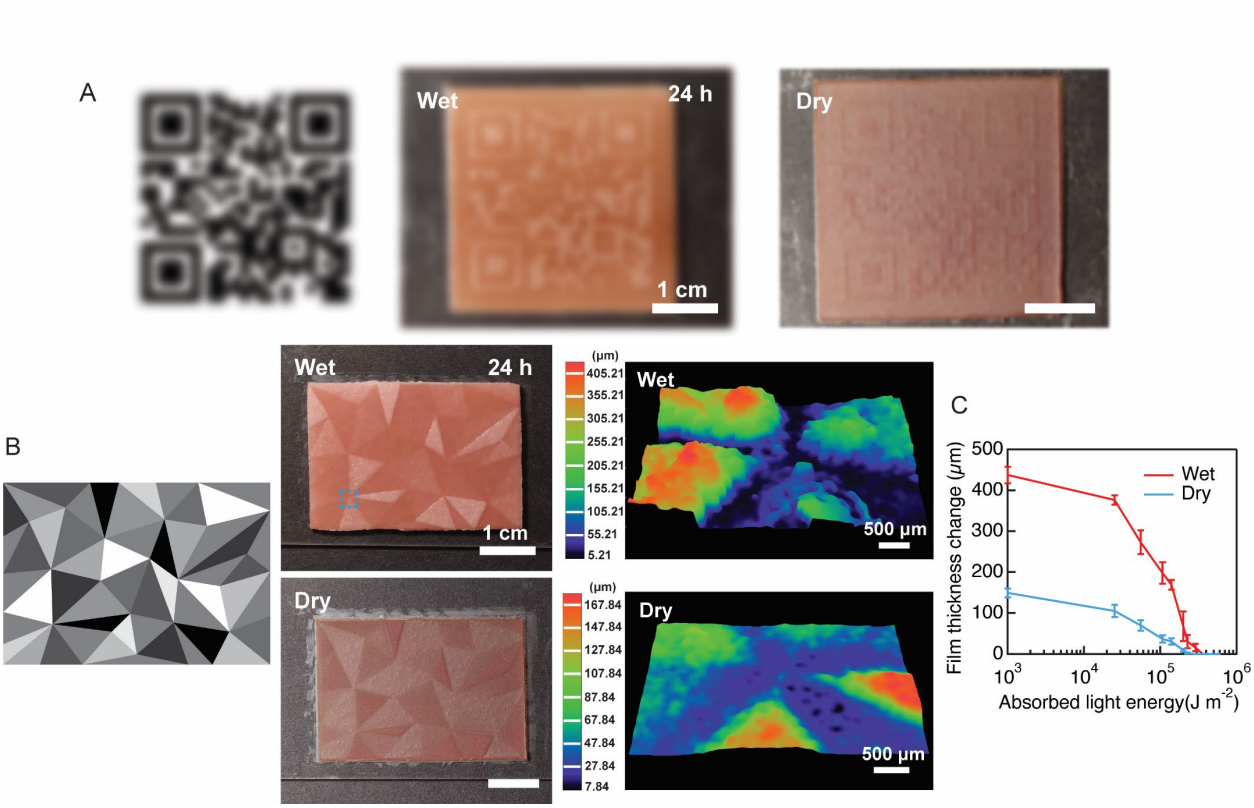

Figure 5. A) A QR code (intentionally blurred) relief surface manufactured and recognized in the wet state, which still retains the shape but becomes unscannable in the dry state (n = 3). B) A grayscale image with varying contrast used as a template to manufacture the relief surface in the wet and dry states. Z-stack optical microscopy heightmap images showing the surface

topography of the wet and dried relief surface at an intersection point in the pattern. C) The effect of absorbed light energy on the resulting grown films thickness change ($n \geq 3$). Each data point represents the mean, and error bars represent SD. Trend lines are only intended to guide the eye.

To explore the potential of this programming strategy, the effect of total irradiated light energy on the thickness change of the grown structures is investigated. As shown in Figure 5B, a grayscale image with 11 contrasts ranging from white to dark was created and projected onto the sample. Notably, the light intensity received by the living film should vary in different contrast areas, resulting in regions with a different extent of inactivation. After programming and growth, the grown films show at least 4 distinct thickness changes in both wet and dry states. Z-stack optical microscopy (OM) images are used to quantify the different film heights (Figure S4, Supporting Information). When the absorbed light energy is below 1,000 J m^{-2}, the film height is relatively unaffected by the incident light (Figure 5C). The film thickness then gradually decreases with an increased dose. There is almost no thickness change during growth when the absorbed light energy is above 288,000 J m^{-2}, indicating a large loss of cell viability. The wet film thickness change ranges from 437.6 ± 20.2 μm to 0 μm in different irradiated areas, while the dry film height ranges from 149.4 ± 11.1 μm to 0 μm. This digital manufacturing strategy is promising for controllable topographical thickness change and may pave the way for future pixel-level gradient relief surfaces manufacturing through the selective growth of living materials (Figure S5, Supporting Information).

3.6. Degradation of living materials. Living materials comprised of high biomass content are well suited to be ultimately degraded after the end of useful life. However, the crosslinked

polymer matrix must also degrade during this process. To enable polymer matrix degradation, the hydrolytically stable crosslinker, MBAm, is replaced with hydrolytically-labile crosslinkers containing aliphatic esters, such as poly(ethylene glycol) diacrylate (PEGDA) or a synthesized ester-containing crosslinker, Bis-PEGDA (**Figure 6**A). Bis-PEGDA is simply synthesized from the Michael addition of 1 equivalent of n-butylamine with 2 equivalents of PEGDA.[73] The resulting mixture of products should be several diacrylates with varying numbers of PEGDA chains connected by β-amino ester linkages.[74] Most of the synthesized product is expected to be two PEGDA molecules linked together. Living materials with the same molar concentration of three different crosslinkers were synthesized and placed in a 33 mM NaOH solution that accelerates hydrolytic degradation. We note that NaOH is not expected to be required for hydrolytic degradation, but that this process will accelerate hydrolysis that would be observed in more neutral conditions.[36,75,76] Here, the accelerated hydrolytic degradation test shows that Bis-PEGDA crosslinked living materials degrade totally, as observed by a total lack of a solid mass, in one day. PEGDA crosslinked living materials degrade within two days, while the dry mass of the MBAm crosslinked living material undergoes very little change (Figure S6, Supporting Information). The relative degradation rates are expected as each MBAm crosslink has no readily hydrolysable bonds, each PEGDA crosslink has two hydrolysable but hindered ester groups,[77,78] and on average each Bis-PEGDA crosslink has four esters with two being readily hydrolysable.[79–81]

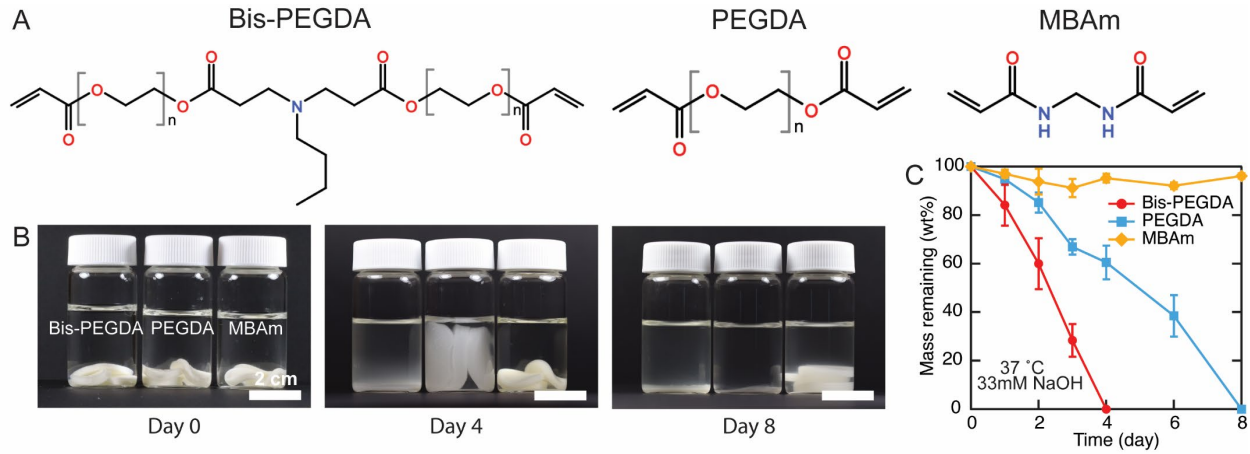

Figure 6. A) Chemical structures of different crosslinkers that are used in the living material system. B) The degradation behavior of the grown living materials by exchanging the crosslinkers in a 33 mM NaOH solution at 37 °C. C) Mass remaining of the three different kinds of grown living materials as a function of time ($n \geq 10$). Each data point represents the mean, and error bars represent SD. Trend lines are only intended to guide the eye.

Biological growth of the living materials does not affect the outcome of degradation but does extend the degradation time. The crosslinker type has no substantial effect on the growth of the living materials (Figure S7, Supporting Information). This indicates that the crosslinkers do not affect cell viability dramatically and that the living materials do not degrade during growth. Under accelerated aging conditions, Bis-PEGDA and PEGDA crosslinked living materials after growth degrade in 4 and 8 days, respectively (Figure 6B and 6C), while MBAm crosslinked grown living materials remain stable in the NaOH solution. Compared with as-synthesized living materials, the degradation rates of grown living materials are slower. One possible reason is that the high cell density of the grown living materials impedes the diffusion of the NaOH solution through the material, resulting in an increased degradation time of the polymer matrix. We note that the water content of the grown gels is lower than that before growth as the dry mass increase

is larger than the volume increase during growth (Figure 1B and 1E). The difference in degradation time between the initial and grown living materials may inspire possible designs of degradable products with spatial-temporal control of degradation time.

4. Conclusion

Manufacturing strategies that use low-energy processes, valorize waste, and result in degradable materials are desired. Our work describes an eco-manufacturing approach where small, programmed preforms comprised of synthetic materials and living cells are fabricated. The growth of embedded cells fueled by bread waste results in a dramatic increase of size and mass of the living materials and the realization of the form of the final object. In the dried state, the grown living materials have elastic moduli in the hundreds of MPa, which can be tuned by both material formulation and the extent of growth. By coupling the dimensional changes due to growth with digital programmability of cell viability, the form of grown objects can greatly exceed the complexity of the initial preform, just as is observed in the morphogenesis of biological tissues. At the end of product life, these grown structures have the capability to degrade hydrolytically. Notably, genetically engineered microorganisms are not encapsulated in the current living material system. Future work with genetically engineered microorganisms may also allow a variety of exciting opportunities for future advanced biomanufacturing of materials.

ASSOCIATED CONTENT

Supporting Information

The following files are available free of charge.

Figure S1. SEM images showing zoom-in views of the dried living materials after growth;

Figure S2. The 3D structure assembled by grown dried living materials supporting a 1 kg weight; **Figure S3.** UV-patterning of the living materials; **Figure S4.** Z-stack optical microscopy images showing surface topography of grown living materials through digital programming; **Figure S5.** The growth behavior of a living material strip using a grayscale image as photopatterning template; **Figure S6.** Degradation behavior of three different kinds of living materials before growth; **Figure S7.** Volume and dry mass change of the living materials with different crosslinkers cultured in bread waste media for 4 days (PDF)

AUTHOR INFORMATION

Corresponding Author

Taylor H. Ware - *Department of Biomedical Engineering, Texas A&M University, College Station, Texas 77840, United States; Department of Materials Science and Engineering, Texas A&M University, College Station, Texas 77840, United States;*

Email: taylor.ware@tamu.edu

Authors

Suitu Wang - *Department of Materials Science and Engineering, Texas A&M University, College Station, Texas 77840, United States;*

Laura K. Rivera-Tarazona - *Department of Biomedical Engineering, Texas A&M University, College Station, Texas 77840, United States;*

Mustafa K. Abdelrahman - *Department of Materials Science and Engineering, Texas A&M University, College Station, Texas 77840, United States;*

Author Contributions

The manuscript was written through contributions of all authors. All authors have given approval to the final version of the manuscript.

Notes

The authors declare no competing financial interest.

ACKNOWLEDGMENT

This material is based upon work supported by the National Science Foundation under Grant No. 2039425. Graphics are created with BioRender.com.

ABBREVIATIONS

ELMs, engineered living materials; HEA, 2-Hydroxyethyl acrylate; AM, acrylamide; MBAm, *N,N′*-methylenebisacrylamide; PEGDA, poly(ethylene glycol) diacrylate; PETMP, pentaerythritol tetrakis(3-mercaptopropionate);TATATO, triallyl isocyanurate; APS, ammonium persulfate; TEMED, N,N,N',N'-tetramethylethane-1,2-diamine; hematoporphyrin, 7,12-*bis*(1-hydroxyethyl)-3,8,13,17-tetramethyl-21H,23H-porphine-2,18-dipropanoic acid, dihydrochloride; YPD, yeast extract-peptone-dextrose; PES, polyethersulfone; DI, deionized water; SEM, scanning electron microscopy; TGA, thermogravimetric analysis; DMA, dynamic mechanical analysis; OM, optical microscopy.

REFERENCES

(1) Rajak, D. K.; Pagar, D. D.; Kumar, R.; Pruncu, C. I. Recent Progress of Reinforcement Materials: A Comprehensive Overview of Composite Materials. *J Mater Res Technology* **2019**, *8* (6), 6354–6374. https://doi.org/10.1016/j.jmrt.2019.09.068.

(2) Ahmad, J. *Machining of Polymer Composites*; Springer; Springer: New York, 2009. https://doi.org/10.1007/978-0-387-68619-6.

(3) Åström, B. T. *Manufacturing of Polymer Composites*; Routledge, 1997. https://doi.org/10.1201/9780203748169.

(4) Zheng, J.; Suh, S. Strategies to Reduce the Global Carbon Footprint of Plastics. *Nat Clim Change* **2019**, *9* (5), 374–378. https://doi.org/10.1038/s41558-019-0459-z.

(5) Geyer, R.; Jambeck, J. R.; Law, K. L. Production, Use, and Fate of All Plastics Ever Made. *Sci Adv* **2017**, *3* (7), e1700782. https://doi.org/10.1126/sciadv.1700782.

(6) Thompson, R. C.; Moore, C. J.; Saal, F. S. vom; Swan, S. H. Plastics, the Environment and Human Health: Current Consensus and Future Trends. *Philosophical Transactions Royal Soc B Biological Sci* **2009**, *364* (1526), 2153–2166. https://doi.org/10.1098/rstb.2009.0053.

(7) Mohanty, A. K.; Vivekanandhan, S.; Pin, J.-M.; Misra, M. Composites from Renewable and Sustainable Resources: Challenges and Innovations. *Science* **2018**, *362* (6414), 536–542. https://doi.org/10.1126/science.aat9072.

(8) Liu, C.; Luan, P.; Li, Q.; Cheng, Z.; Sun, X.; Cao, D.; Zhu, H. Biodegradable, Hygienic, and Compostable Tableware from Hybrid Sugarcane and Bamboo Fibers as Plastic Alternative. *Matter* **2020**, *3* (6), 2066–2079. https://doi.org/10.1016/j.matt.2020.10.004.

(9) Wang, J.; Zhang, D.; Chu, F. Wood-Derived Functional Polymeric Materials. *Adv Mater* **2020**, 2001135. https://doi.org/10.1002/adma.202001135.

(10) Schneiderman, D. K.; Hillmyer, M. A. 50th Anniversary Perspective : There Is a Great Future in Sustainable Polymers. *Macromolecules* **2017**, *50* (10), 3733–3749. https://doi.org/10.1021/acs.macromol.7b00293.

(11) Yang, Y.; Song, X.; Li, X.; Chen, Z.; Zhou, C.; Zhou, Q.; Chen, Y. Recent Progress in Biomimetic Additive Manufacturing Technology: From Materials to Functional Structures. *Adv Mater* **2018**, *30* (36), 1706539. https://doi.org/10.1002/adma.201706539.

(12) Velasco-Hogan, A.; Xu, J.; Meyers, M. A. Additive Manufacturing as a Method to Design and Optimize Bioinspired Structures. *Adv Mater* **2018**, *30* (52), 1800940. https://doi.org/10.1002/adma.201800940.

(13) Gross, R. A.; Kalra, B. Biodegradable Polymers for the Environment. *Science* **2002**, *297* (5582), 803–807. https://doi.org/10.1126/science.297.5582.803.

(14) Chiellini, E.; Solaro, R. Biodegradable Polymeric Materials. *Adv Mater* **1996**, *8* (4), 305–313. https://doi.org/10.1002/adma.19960080406.

(15) Melikoglu, M.; Webb, C. Food Industry Wastes. *Part Ii Treat Solid Food Wastes* **2013**, 63–76. https://doi.org/10.1016/b978-0-12-391921-2.00004-4.

(16) Leung, C. C. J.; Cheung, A. S. Y.; Zhang, A. Y.-Z.; Lam, K. F.; Lin, C. S. K. Utilisation of Waste Bread for Fermentative Succinic Acid Production. *Biochem Eng J* **2012**, *65*, 10–15. https://doi.org/10.1016/j.bej.2012.03.010.

(17) Oda, Y.; Park, B.-S.; Moon, K.-H.; Tonomura, K. Recycling of Bakery Wastes Using an Amylolytic Lactic Acid Bacterium. *Bioresource Technol* **1997**, *60* (2), 101–106. https://doi.org/10.1016/s0960-8524(97)00008-4.

(18) Pietrzak, W.; Kawa-Rygielska, J. Ethanol Fermentation of Waste Bread Using Granular Starch Hydrolyzing Enzyme: Effect of Raw Material Pretreatment. *Fuel* **2014**, *134*, 250–256. https://doi.org/10.1016/j.fuel.2014.05.081.

(19) Cerda, A.; El-Bakry, M.; Gea, T.; Sánchez, A. Long Term Enhanced Solid-State Fermentation: Inoculation Strategies for Amylase Production from Soy and Bread Wastes by Thermomyces Sp. in a Sequential Batch Operation. *J Environ Chem Eng* **2016**, *4* (2), 2394–2401. https://doi.org/10.1016/j.jece.2016.04.022.

(20) Benabda, O.; Kasmi, M.; Kachouri, F.; Hamdi, M. Valorization of the Powdered Bread Waste Hydrolysate as Growth Medium for Baker Yeast. *Food Bioprod Process* **2018**, *109*, 1–8. https://doi.org/10.1016/j.fbp.2018.02.007.

(21) Verni, M.; Minisci, A.; Convertino, S.; Nionelli, L.; Rizzello, C. G. Wasted Bread as Substrate for the Cultivation of Starters for the Food Industry. *Front Microbiol* **2020**, *11*, 293. https://doi.org/10.3389/fmicb.2020.00293.

(22) Tofail, S. A. M.; Koumoulos, E. P.; Bandyopadhyay, A.; Bose, S.; O'Donoghue, L.; Charitidis, C. Additive Manufacturing: Scientific and Technological Challenges, Market Uptake and Opportunities. *Mater Today* **2018**, *21* (1), 22–37. https://doi.org/10.1016/j.mattod.2017.07.001.

(23) Studart, A. R. Additive Manufacturing of Biologically-Inspired Materials. *Chem Soc Rev* **2016**, *45* (2), 359–376. https://doi.org/10.1039/c5cs00836k.

(24) Chen, A. Y.; Zhong, C.; Lu, T. K. Engineering Living Functional Materials. *Acs Synth Biol* **2015**, *4* (1), 8–11. https://doi.org/10.1021/sb500113b.

(25) Nguyen, P. Q.; Courchesne, N.-M. D.; Duraj-Thatte, A.; Praveschotinunt, P.; Joshi, N. S. Engineered Living Materials: Prospects and Challenges for Using Biological Systems to Direct the Assembly of Smart Materials. *Adv Mater* **2018**, *30* (19), 1704847. https://doi.org/10.1002/adma.201704847.

(26) Gilbert, C.; Ellis, T. Biological Engineered Living Materials: Growing Functional Materials with Genetically Programmable Properties. *Acs Synth Biol* **2019**, *8* (1), 1–15. https://doi.org/10.1021/acssynbio.8b00423.

(27) Rivera-Tarazona, L. K.; Campbell, Z. T.; Ware, T. H. Stimuli-Responsive Engineered Living Materials. *Soft Matter* **2020**, *17* (4), 785–809. https://doi.org/10.1039/d0sm01905d.

(28) Srubar, W. V. Engineered Living Materials: Taxonomies and Emerging Trends. *Trends Biotechnol* **2020**, *39* (6), 574–583. https://doi.org/10.1016/j.tibtech.2020.10.009.

(29) Molinari, S.; Tesoriero, R. F.; Ajo-Franklin, C. M. Bottom-up Approaches to Engineered Living Materials: Challenges and Future Directions. *Matter* **2021**, *4* (10), 3095–3120. https://doi.org/10.1016/j.matt.2021.08.001.

(30) Rodrigo-Navarro, A.; Sankaran, S.; Dalby, M. J.; Campo, A. del; Salmeron-Sanchez, M. Engineered Living Biomaterials. *Nat Rev Mater* **2021**, *6* (12), 1175–1190. https://doi.org/10.1038/s41578-021-00350-8.

(31) Rivera-Tarazona, L. K.; Shukla, T.; Singh, K. A.; Gaharwar, A. K.; Campbell, Z. T.; Ware, T. H. 4D Printing of Engineered Living Materials. *Adv Funct Mater* **2022**, *32* (4), 2106843. https://doi.org/10.1002/adfm.202106843.

(32) González, L. M.; Mukhitov, N.; Voigt, C. A. Resilient Living Materials Built by Printing Bacterial Spores. *Nat Chem Biol* **2020**, *16* (2), 126–133. https://doi.org/10.1038/s41589-019-0412-5.

(33) Caro-Astorga, J.; Walker, K. T.; Herrera, N.; Lee, K.-Y.; Ellis, T. Bacterial Cellulose Spheroids as Building Blocks for 3D and Patterned Living Materials and for Regeneration. *Nat Commun* **2021**, *12* (1), 5027. https://doi.org/10.1038/s41467-021-25350-8.

(34) An, B.; Wang, Y.; Jiang, X.; Ma, C.; Mimee, M.; Moser, F.; Li, K.; Wang, X.; Tang, T.-C.; Huang, Y.; Liu, Y.; Lu, T. K.; Zhong, C. Programming Living Glue Systems to Perform Autonomous Mechanical Repairs. *Matter* **2020**, *3* (6), 2080–2092. https://doi.org/10.1016/j.matt.2020.09.006.

(35) Huang, J.; Liu, S.; Zhang, C.; Wang, X.; Pu, J.; Ba, F.; Xue, S.; Ye, H.; Zhao, T.; Li, K.; Wang, Y.; Zhang, J.; Wang, L.; Fan, C.; Lu, T. K.; Zhong, C. Programmable and Printable Bacillus Subtilis Biofilms as Engineered Living Materials. *Nat Chem Biol* **2019**, *15* (1), 34–41. https://doi.org/10.1038/s41589-018-0169-2.

(36) Feng, J.; Zheng, Y.; Bhusari, S.; Villiou, M.; Pearson, S.; Campo, A. Printed Degradable Optical Waveguides for Guiding Light into Tissue. *Adv Funct Mater* **2020**, *30* (45), 2004327. https://doi.org/10.1002/adfm.202004327.

(37) Gerber, L. C.; Koehler, F. M.; Grass, R. N.; Stark, W. J. Incorporating Microorganisms into Polymer Layers Provides Bioinspired Functional Living Materials. *Proc National Acad Sci* **2012**, *109* (1), 90–94. https://doi.org/10.1073/pnas.1115381109.

(38) Freyman, M. C.; Kou, T.; Wang, S.; Li, Y. 3D Printing of Living Bacteria Electrode. *Nano Res* **2020**, *13* (5), 1318–1323. https://doi.org/10.1007/s12274-019-2534-1.

(39) Saha, A.; Johnston, T. G.; Shafranek, R. T.; Goodman, C. J.; Zalatan, J. G.; Storti, D. W.; Ganter, M. A.; Nelson, A. Additive Manufacturing of Catalytically Active Living Materials. *Acs Appl Mater Inter* **2018**, *10* (16), 13373–13380. https://doi.org/10.1021/acsami.8b02719.

(40) Liu, X.; Tang, T.-C.; Tham, E.; Yuk, H.; Lin, S.; Lu, T. K.; Zhao, X. Stretchable Living Materials and Devices with Hydrogel–Elastomer Hybrids Hosting Programmed Cells. *Proc National Acad Sci* **2017**, *114* (9), 2200–2205. https://doi.org/10.1073/pnas.1618307114.

(41) Kwak, S.-Y.; Giraldo, J. P.; Lew, T. T. S.; Wong, M. H.; Liu, P.; Yang, Y. J.; Koman, V. B.; McGee, M. K.; Olsen, B. D.; Strano, M. S. Polymethacrylamide and Carbon Composites That Grow, Strengthen, and Self-Repair Using Ambient Carbon Dioxide Fixation. *Adv Mater* **2018**, *30* (46), 1804037. https://doi.org/10.1002/adma.201804037.

(42) Yu, K.; Feng, Z.; Du, H.; Xin, A.; Lee, K. H.; Li, K.; Su, Y.; Wang, Q.; Fang, N. X.; Daraio, C. Photosynthesis-Assisted Remodeling of Three-Dimensional Printed Structures. *Proc National Acad Sci* **2021**, *118* (3), e2016524118. https://doi.org/10.1073/pnas.2016524118.

(43) Kang, S.-Y.; Pokhrel, A.; Bratsch, S.; Benson, J. J.; Seo, S.-O.; Quin, M. B.; Aksan, A.; Schmidt-Dannert, C. Engineering Bacillus Subtilis for the Formation of a Durable Living Biocomposite Material. *Nat Commun* **2021**, *12* (1), 7133. https://doi.org/10.1038/s41467-021-27467-2.

(44) Johnston, T. G.; Yuan, S.-F.; Wagner, J. M.; Yi, X.; Saha, A.; Smith, P.; Nelson, A.; Alper, H. S. Compartmentalized Microbes and Co-Cultures in Hydrogels for on-Demand Bioproduction and Preservation. *Nat Commun* **2020**, *11* (1), 563. https://doi.org/10.1038/s41467-020-14371-4.

(45) McBee, R. M.; Lucht, M.; Mukhitov, N.; Richardson, M.; Srinivasan, T.; Meng, D.; Chen, H.; Kaufman, A.; Reitman, M.; Munck, C.; Schaak, D.; Voigt, C.; Wang, H. H. Engineering Living and Regenerative Fungal–Bacterial Biocomposite Structures. *Nat Mater* **2021**, 1–8. https://doi.org/10.1038/s41563-021-01123-y.

(46) Manjula-Basavanna, A.; Duraj-Thatte, A. M.; Joshi, N. S. Robust Self-Regeneratable Stiff Living Materials Fabricated from Microbial Cells. *Adv Funct Mater* **2021**, 2010784. https://doi.org/10.1002/adfm.202010784.

(47) Vallas, T.; Courard, L. Using Nature in Architecture: Building a Living House with Mycelium and Trees. *Frontiers Archit Res* **2017**, *6* (3), 318–328. https://doi.org/10.1016/j.foar.2017.05.003.

(48) Jones, M.; Mautner, A.; Luenco, S.; Bismarck, A.; John, S. Engineered Mycelium Composite Construction Materials from Fungal Biorefineries: A Critical Review. *Mater Design* **2019**, *187*, 108397. https://doi.org/10.1016/j.matdes.2019.108397.

(49) Elsacker, E.; Søndergaard, A.; Wylick, A. V.; Peeters, E.; Laet, L. D. Growing Living and Multifunctional Mycelium Composites for Large-Scale Formwork Applications Using Robotic Abrasive Wire-Cutting. *Constr Build Mater* **2021**, *283*, 122732. https://doi.org/10.1016/j.conbuildmat.2021.122732.

(50) Xin, A.; Su, Y.; Feng, S.; Yan, M.; Yu, K.; Feng, Z.; Lee, K. H.; Sun, L.; Wang, Q. Growing Living Composites with Ordered Microstructures and Exceptional Mechanical Properties. *Adv Mater* **2021**, 2006946. https://doi.org/10.1002/adma.202006946.

(51) Duraj-Thatte, A. M.; Manjula-Basavanna, A.; Courchesne, N.-M. D.; Cannici, G. I.; Sánchez-Ferrer, A.; Frank, B. P.; Hag, L. V.; Cotts, S. K.; Fairbrother, D. H.; Mezzenga, R.; Joshi, N. S. Water-Processable, Biodegradable and Coatable Aquaplastic from Engineered Biofilms. *Nat Chem Biol* **2021**, *17* (6), 732–738. https://doi.org/10.1038/s41589-021-00773-y.

(52) Gilbert, C.; Tang, T.-C.; Ott, W.; Dorr, B. A.; Shaw, W. M.; Sun, G. L.; Lu, T. K.; Ellis, T. Living Materials with Programmable Functionalities Grown from Engineered Microbial Co-Cultures. *Nat Mater* **2021**, 1–10. https://doi.org/10.1038/s41563-020-00857-5.

(53) Rivera-Tarazona, L. K.; Bhat, V. D.; Kim, H.; Campbell, Z. T.; Ware, T. H. Shape-Morphing Living Composites. *Sci Adv* **2020**, *6* (3), eaax8582. https://doi.org/10.1126/sciadv.aax8582.

(54) Stenson, J. D.; Hartley, P.; Wang, C.; Thomas, C. R. Determining the Mechanical Properties of Yeast Cell Walls. *Biotechnol Progr* **2011**, *27* (2), 505–512. https://doi.org/10.1002/btpr.554.

(55) Siess, M. H.; Divies, C. Behaviour of Saccharomyces Cerevisiae Cells Entrapped in a Polyacrylamide Gel and Performing Alcoholic Fermentation. *Eur J Appl Microbiol* **1981**, *12* (1), 10–15. https://doi.org/10.1007/bf00508112.

(56) Pines, G.; Freeman, A. Immobilization and Characterization of Saccharomyces Cerevisiae in Crosslinked, Prepolymerized Polyacrylamide-Hydrazide. *Eur J Appl Microbiol* **1982**, *16* (2–3), 75–80. https://doi.org/10.1007/bf00500730.

(57) Burrill, H. N.; Bell, L. E.; Greenfield, P. F.; Do, D. D. Analysis of Distributed Growth of Saccharomyces Cerevisiae Cells Immobilized in Polyacrylamide Gel. *Appl Environ Microb* **1983**, *46* (3), 716–721. https://doi.org/10.1128/aem.46.3.716-721.1983.

(58) Karel, S. F.; Libicki, S. B.; Robertson, C. R. The Immobilization of Whole Cells: Engineering Principles. *Chem Eng Sci* **1985**, *40* (8), 1321–1354. https://doi.org/10.1016/0009-2509(85)80074-9.

(59) Pradas, M. M.; Ribelles, J. L. G.; Aroca, A. S.; Ferrer, G. G.; Antón, J. S.; Pissis, P. Porous Poly(2-Hydroxyethyl Acrylate) Hydrogels. *Polymer* **2001**, *42* (10), 4667–4674. https://doi.org/10.1016/s0032-3861(00)00742-4.

(60) Ejeromedoghene, O.; Hu, Y. P.; Oderinde, O.; Yao, F.; Akinremi, C.; Akinyeye, R.; Adewuyi, S.; Fu, G. Transparent and Photochromic Poly(Hydroxyethyl Acrylate–Acrylamide)/WO3 Hydrogel with Antibacterial Properties against Bacterial Keratitis in Contact Lens. *J Appl Polym Sci* **2022**, *139* (12). https://doi.org/10.1002/app.51815.

(61) Li, Z.; Liu, Z.; Ng, T. Y.; Sharma, P. The Effect of Water Content on the Elastic Modulus and Fracture Energy of Hydrogel. *Extreme Mech Lett* **2020**, *35*, 100617. https://doi.org/10.1016/j.eml.2019.100617.

(62) Li, A.; Ramakrishna, S. N.; Kooij, E. S.; Espinosa-Marzal, R. M.; Spencer, N. D. Poly(Acrylamide) Films at the Solvent -Induced Glass Transition: Adhesion, Tribology, and the Influence of Crosslinking. *Soft Matter* **2012**, *8* (35), 9092–9100. https://doi.org/10.1039/c2sm26222c.

(63) Smith, A. E.; Zhang, Z.; Thomas, C. R.; Moxham, K. E.; Middelberg, A. P. J. The Mechanical Properties of Saccharomyces Cerevisiae. *Proc National Acad Sci* **2000**, *97* (18), 9871–9874. https://doi.org/10.1073/pnas.97.18.9871.

(64) Beker, M. J.; Rapoport, A. I. Biotechnology Methods. *Adv Biochem Eng Biotechnology* **2005**, 127–171. https://doi.org/10.1007/bfb0004428.

(65) Klein, Y.; Efrati, E.; Sharon, E. Shaping of Elastic Sheets by Prescription of Non-Euclidean Metrics. *Science* **2007**, *315* (5815), 1116–1120. https://doi.org/10.1126/science.1135994.

(66) Kim, J.; Hanna, J. A.; Byun, M.; Santangelo, C. D.; Hayward, R. C. Designing Responsive Buckled Surfaces by Halftone Gel Lithography. *Science* **2012**, *335* (6073), 1201–1205. https://doi.org/10.1126/science.1215309.

(67) Gladman, A. S.; Matsumoto, E. A.; Nuzzo, R. G.; Mahadevan, L.; Lewis, J. A. Biomimetic 4D Printing. *Nat Mater* **2016**, *15* (4), 413–418. https://doi.org/10.1038/nmat4544.

(68) Nojoomi, A.; Arslan, H.; Lee, K.; Yum, K. Bioinspired 3D Structures with Programmable Morphologies and Motions. *Nat Commun* **2018**, *9* (1), 3705. https://doi.org/10.1038/s41467-018-05569-8.

(69) Jori, G.; Fabris, C.; Soncin, M.; Ferro, S.; Coppellotti, O.; Dei, D.; Fantetti, L.; Chiti, G.; Roncucci, G. Photodynamic Therapy in the Treatment of Microbial Infections: Basic Principles and Perspective Applications. *Laser Surg Med* **2006**, *38* (5), 468–481. https://doi.org/10.1002/lsm.20361.

(70) Donnelly, R. F.; McCarron, P. A.; Tunney, M. M. Antifungal Photodynamic Therapy. *Microbiol Res* **2008**, *163* (1), 1–12. https://doi.org/10.1016/j.micres.2007.08.001.

(71) Ito, T. PHOTODYNAMIC ACTION OF HEMATOPORPHYRIN ON YEAST CELLS—A KINETIC APPROACH. *Photochem Photobiol* **1981**, *34* (4), 521–524. https://doi.org/10.1111/j.1751-1097.1981.tb09035.x.

(72) Stenstrøm, A. G. K.; Moan, J.; Brunborg, G.; Eklund, T. PHOTODYNAMIC INACTIVATION OF YEAST CELLS SENSITIZED BY HEMATOPORPHYRIN. *Photochem Photobiol* **1980**, *32* (3), 349–352. https://doi.org/10.1111/j.1751-1097.1980.tb03773.x.

(73) Safranski, D. L.; Weiss, D.; Clark, J. B.; Caspersen, B. S.; Taylor, W. R.; Gall, K. Effect of Poly(Ethylene Glycol) Diacrylate Concentration on Network Properties and in Vivo Response of Poly(B-amino Ester) Networks. *J Biomed Mater Res A* **2011**, *96A* (2), 320–329. https://doi.org/10.1002/jbm.a.32983.

(74) Liu, Y.; Li, Y.; Keskin, D.; Shi, L. Poly(B-Amino Esters): Synthesis, Formulations, and Their Biomedical Applications. *Adv Healthc Mater* **2019**, *8* (2), 1801359. https://doi.org/10.1002/adhm.201801359.

(75) Browning, M. B.; Cereceres, S. N.; Luong, P. T.; Cosgriff-Hernandez, E. M. Determination of the in Vivo Degradation Mechanism of PEGDA Hydrogels. *J Biomed Mater Res A* **2014**, *102* (12), 4244–4251. https://doi.org/10.1002/jbm.a.35096.

(76) Maeng, J.; Rihani, R. T.; Javed, M.; Rajput, J. S.; Kim, H.; Bouton, I. G.; Criss, T. A.; Pancrazio, J. J.; Black, B. J.; Ware, T. H. Liquid Crystal Elastomers as Substrates for 3D, Robust, Implantable Electronics. *J Mater Chem B* **2020**, *8* (29), 6286–6295. https://doi.org/10.1039/d0tb00471e.

(77) Browning, M. B.; Cosgriff-Hernandez, E. Development of a Biostable Replacement for PEGDA Hydrogels. *Biomacromolecules* **2012**, *13* (3), 779–786. https://doi.org/10.1021/bm201707z.

(78) Cereceres, S.; Lan, Z.; Bryan, L.; Whitely, M.; Wilems, T.; Fabela, N.; Whitfield-Cargile, C.; Cosgriff-Hernandez, E. In Vivo Characterization of Poly(Ethylene Glycol) Hydrogels with Thio-β Esters. *Ann Biomed Eng* **2020**, *48* (3), 953–967. https://doi.org/10.1007/s10439-019-02271-8.

(79) McBath, R. A.; Shipp, D. A. Swelling and Degradation of Hydrogels Synthesized with Degradable Poly(β-Amino Ester) Crosslinkers. *Polym Chem-uk* **2010**, *1* (6), 860–865. https://doi.org/10.1039/c0py00074d.

(80) Hawkins, A. M.; Puleo, D. A.; Hilt, J. Z. Effect of Macromer Synthesis Time on the Properties of the Resulting Poly(B-amino Ester) Degradable Hydrogel. *J Appl Polym Sci* **2011**, *122* (2), 1420–1426. https://doi.org/10.1002/app.34093.

(81) Hawkins, A. M.; Milbrandt, T. A.; Puleo, D. A.; Hilt, J. Z. Synthesis and Analysis of Degradation, Mechanical and Toxicity Properties of Poly(β-Amino Ester) Degradable Hydrogels. *Acta Biomater* **2011**, *7* (5), 1956–1964. https://doi.org/10.1016/j.actbio.2011.01.024.

For Table of Contents Only